

Development of Aluminum Honeycomb Model Using Shell Elements

Shigeki Kojima

Toyota Technical Development Corporation, Japan

Tsuyoshi Yasuki

Toyota Motor Corporation, Japan

Abstract

This paper describes a new finite element modeling method of aluminum honeycomb using shell elements. It is our new modeling method that cell size of honeycomb structure is enlarged to keep minimum mesh size, and compressive strength is controlled by thickness of shell elements.

New modeling was applied to an offset deformable barrier model, and full vehicle crash analysis was performed.

The result of offset frontal collision analysis with a new honeycomb model showed much better correlation with test results than with modified material type-126 solid elements.

1. Introduction

In using offset frontal collision analysis to predict the amount of vehicle deformation, it is essential for the offset deformable barrier (ODB) model to replicate the compressive property and deformed shape of aluminum honeycomb accurately. Currently, aluminum honeycomb has been modeled using solid elements, and the prediction accuracy of FEM analysis has been improved by modification of the material model.

This paper describes a method of modeling aluminum honeycomb using shell elements, which was developed to further improve the prediction accuracy of FEM analysis. A shell element ODB model was then used in offset frontal collision analysis, and the prediction accuracy for the deformed shape of the vehicle and ODB was verified.

2. Motivation of Study

2.1 Comparison of test results and FEM analysis for offset frontal collision

Offset frontal collision analysis was performed using a solid element ODB model and vehicle model. Figure 1 shows the deformed shape of the vehicle after the collision and Fig. 2 shows that of the ODB. MAT126, with additional function over V970 Revision5434, was used as the aluminum honeycomb material model for the ODB model.

In the FEM analysis, the remaining crushed portion of the upper member was 33 mm larger than that shown by the test results. On the other hand, the remaining crushed portion of the upper part of the ODB core honeycomb where the upper member collided was 59 mm smaller than that shown by the test results. Thus differences are observed between the test results and the FEM analysis in the deformation modes.

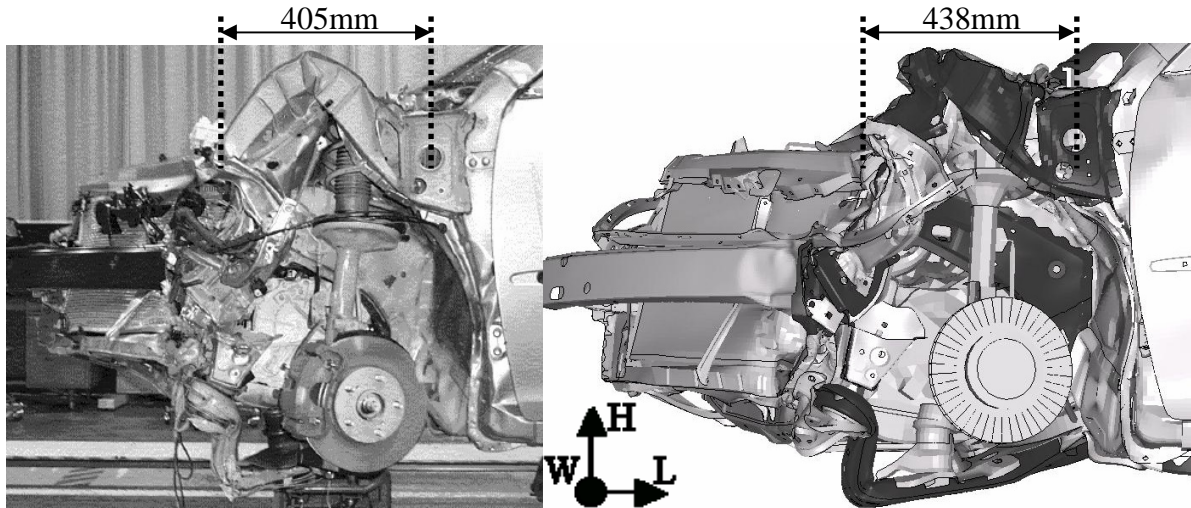


Fig.1 Deformed shape of vehicle after offset frontal collision

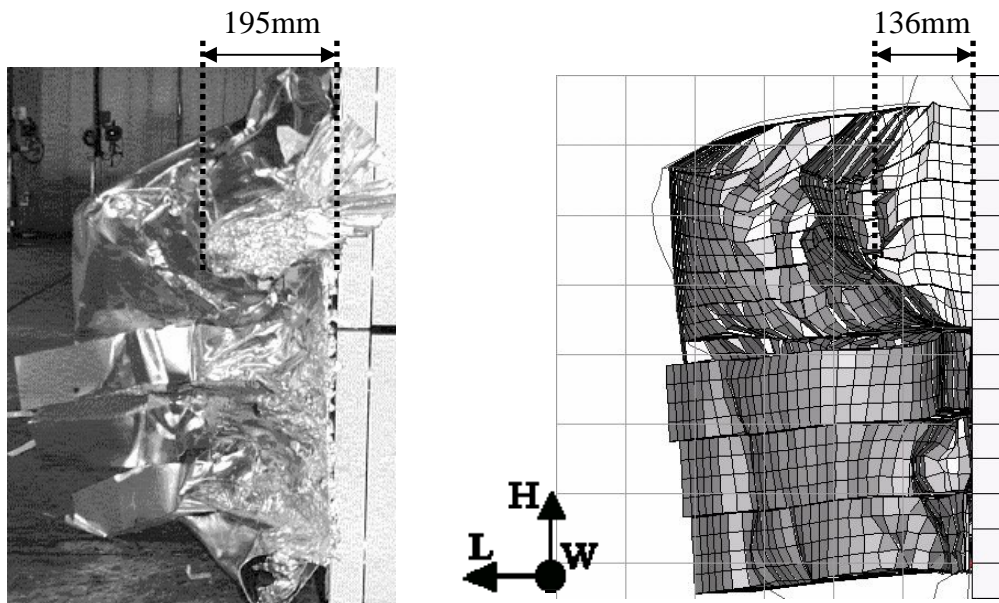
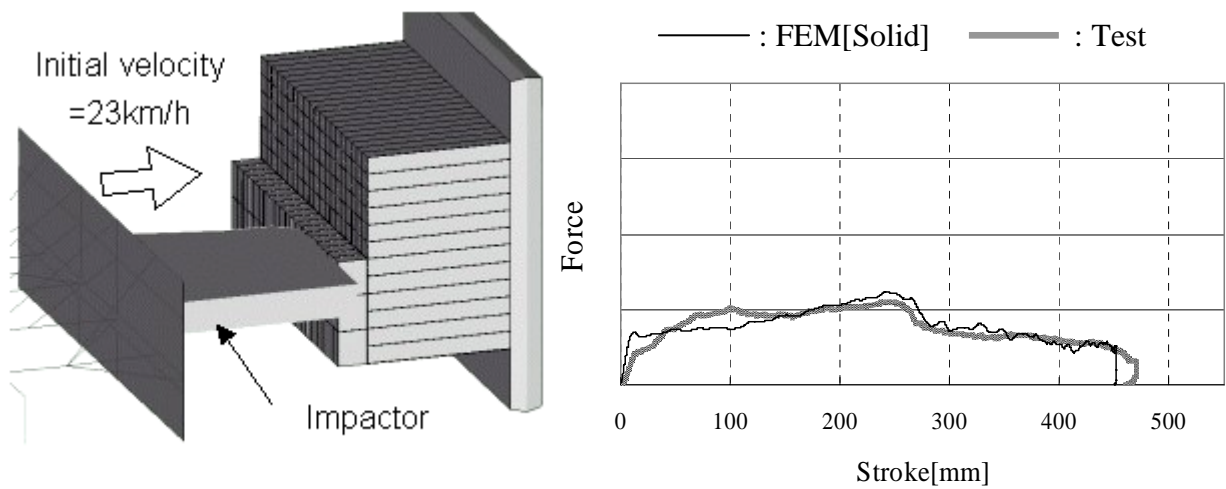


Fig.2 Deformed shape of ODB after offset frontal collision

2.2 Comparison of test results and FEM analysis for barrier inspection.

To verify the accuracy of the deformation mode of the solid element ODB model, a barrier inspection analysis was performed using a rigid impactor and the solid element ODB model. Figure 3(a) shows an outline of the FEM analysis for barrier inspection, and Fig. 3(b) shows the relationship between impactor stroke and barrier force. Figure 4 shows the deformed shape of the ODB after the collision.

The relationship between impactor stroke and barrier force using the solid element ODB model generally matched the test results. However, when the deformed shape of the core honeycomb was examined after the collision test, it was found that the cladding sheet had become entangled into the impactor, and the core honeycomb was gathered to the impactor side. In the solid element ODB model, on the other hand, a different deformed shape was obtained. In this case, the upper and lower portions of the core honeycomb were gathered into the center, separated by the impactor.



(a) Impactor test FE model

(b) Comparison of Force-Stroke curves

Fig.3 Impactor test

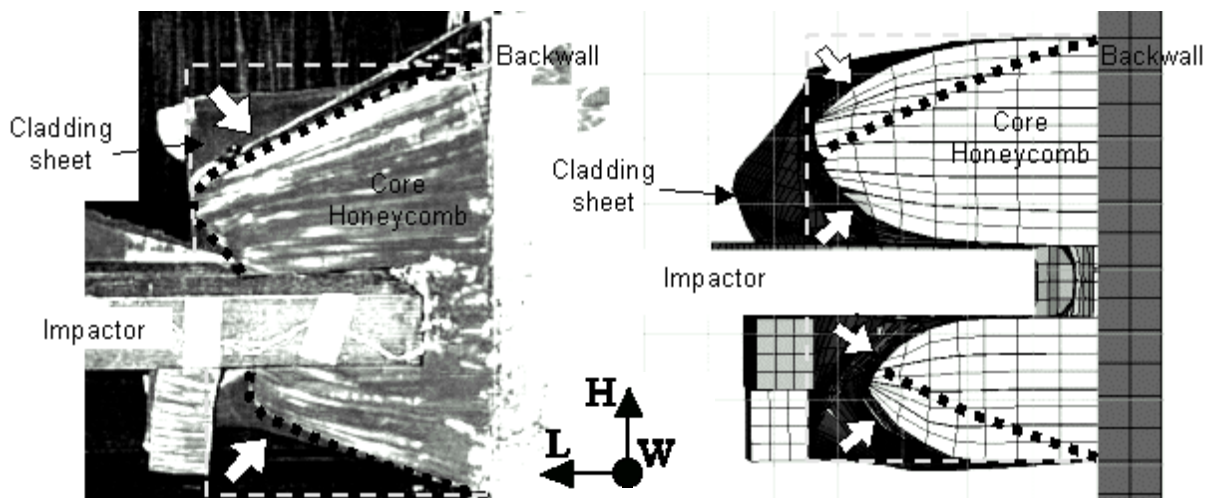


Fig.4 Deformed shape of ODB after impactor collision

2.3 Cause of difference in deformed shape of core honeycomb

This section examines the cause of the difference in the deformed shape of the core honeycomb in the ODB barrier inspection. Figure 5(a) shows the deformed shape of the barrier, and Fig. 5(b) shows the hourglass deformation of the solid elements predicted by the FEM analysis. Figure 6 shows the time history of energy in the core honeycomb region A. In the core honeycomb region A, hourglass energy is generated equivalent to 95% of the internal energy. One of the causes of the difference with the test results is the hourglass control performed over the solid elements simulating the core honeycomb. It was therefore assumed that the difference with the test was caused by the effect of non-physical hourglass control suppressing collapse deformation at the upper end of the core honeycomb.

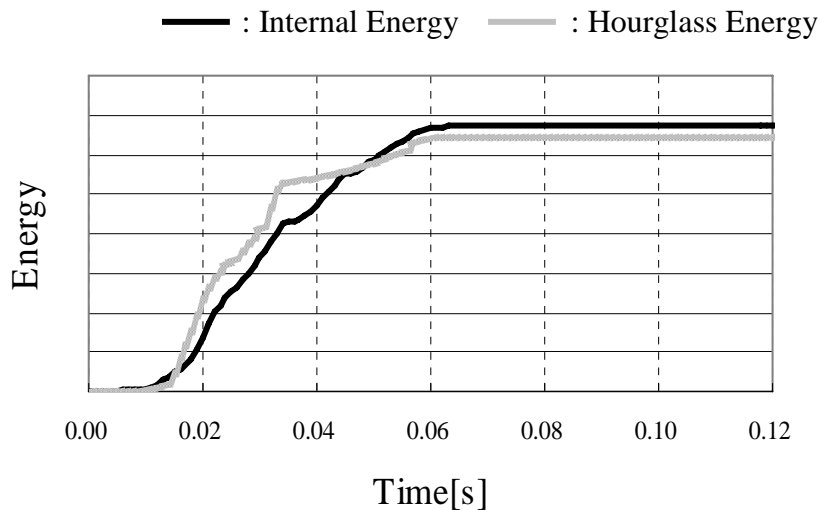
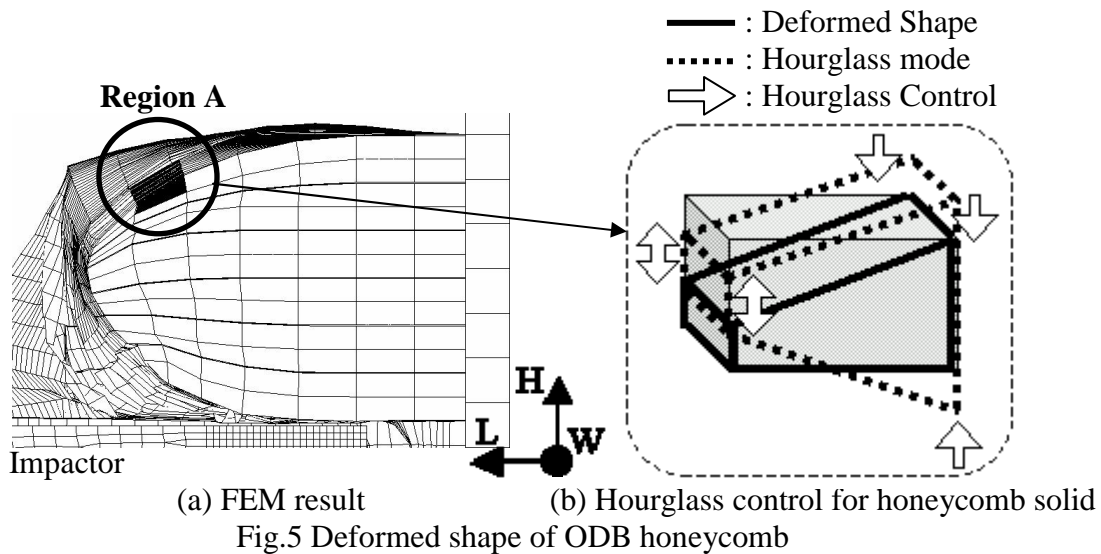


Fig.6 Time history of energy in core honeycomb region A

3. Honeycomb Modeling

3.1 Modeling of Aluminum honeycomb using shell elements

Hourglass control is always applied to one-point integration solid elements for an aluminum honeycomb model. Therefore, to avoid the hourglass control over the solid elements, the modeling of the aluminum honeycomb was reviewed, and an aluminum honeycomb model based on shell elements was developed.

However, the cell size in the ODB core honeycomb is 19.1 mm, and when one side of a hexagon is split into three elements, the size of each element becomes 1 to 2 mm, meaning that tens of millions of shell elements will be required for an entire ODB. Since it is currently difficult to perform calculations for a large-scale model consisting of even tens of thousands of elements, a unique honeycomb modeling method with a reduced number of elements was developed.

Figure 7 shows the shell element aluminum honeycomb model developed in this paper. In the FEM model, the cell size of the ODB core honeycomb was increased from 19.1 mm to 34.6 mm, and the minimum length of a shell element was set at 5 mm to reduce the number of elements.

Moreover, the thickness of the shell elements parallel to the LH plane was defined as twice the thickness of the diagonally positioned elements in order to simulate the bonding portions of the aluminum plates that comprise the honeycomb.

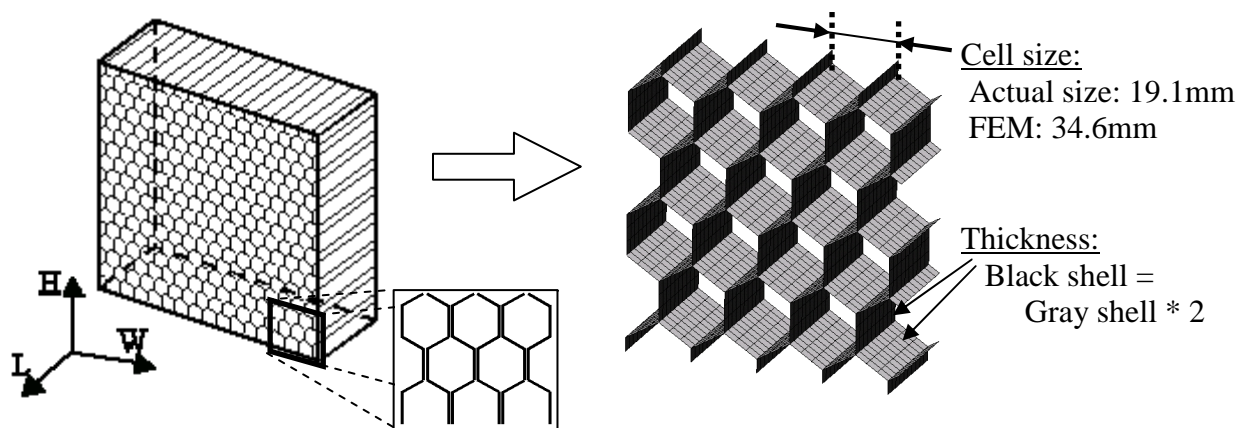


Fig.7 Modeling method of aluminum honeycomb

Increasing the cell size of the aluminum honeycomb model causes a difference with the actual part in terms of compressive strength. Therefore, the compressive strength of the actual part was reproduced by defining a virtual thickness. To obtain the relationship between the thickness of shell elements comprising a honeycomb and compressive strength, a parameter study using a test piece was performed. Figure 8(a) shows an outline of the test piece compression model, and Fig. 8(b) shows the relationship between the thickness of honeycomb shell elements and compressive stress. An aluminum honeycomb model was created by determining the shell thickness based on the curve shown in (b), which was then incorporated into the ODB model.

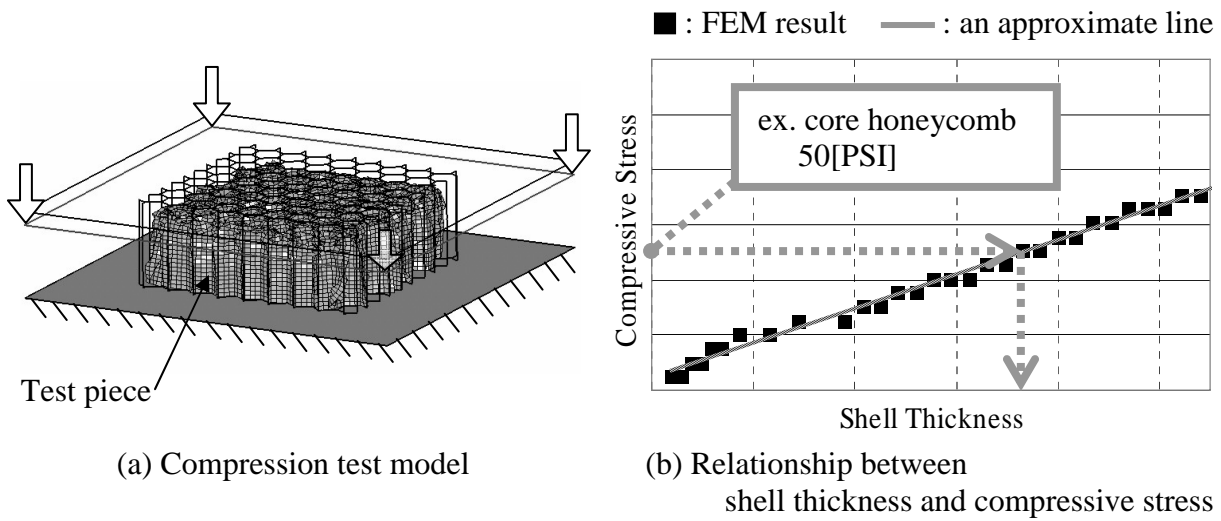


Fig.8 Compression test of aluminum honeycomb

3.2 Pre-crashed structure of Aluminum honeycomb and adhesive model

Figure 9(a) shows an outline of the shell element ODB model, and Fig. 9(b) shows the pre-crashed structure of the core honeycomb and the modeling of the adhesive with the cladding sheet. To approximate the shape of the actual part, pre-crashed areas were applied at the ends of the ODB core honeycomb. Furthermore, with regard to the bonding between the aluminum honeycomb and cladding sheet, beam elements were used to simulate the rupturing of the adhesive.

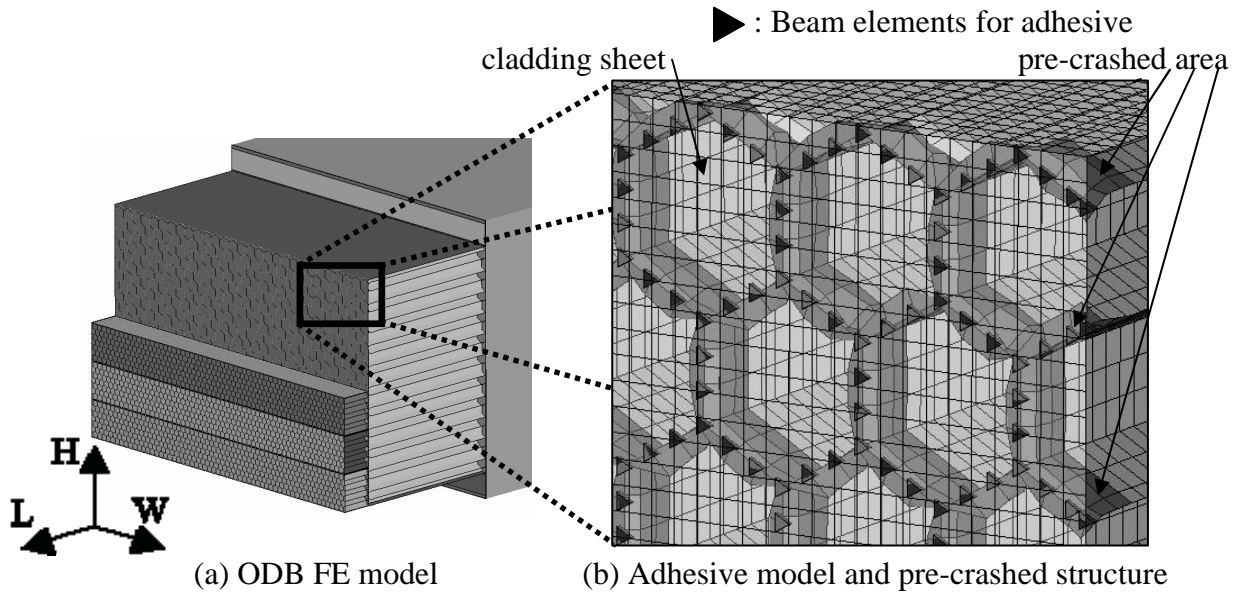


Fig.9 ODB FE model using shell elements

4. Results

4.1 Verification of directional dependence of Aluminum honeycomb compressive strength

The directional dependence of compressive strength was tested to verify the calculation accuracy of the newly created shell element aluminum honeycomb model. 150x150x50 mm test pieces were cut out from the ODB core honeycomb at various angles in increments of 10 degrees with respect to the W axis, and static compression tests performed. Figure 10 shows an outline of the compression test on the aluminum honeycomb test pieces, and Fig. 11 indicates the relationship between compressive stress and the test piece cut-out angle with a stroke of 10 mm.

The relationship between the compressive stress of the shell element aluminum honeycomb model and the test piece cut-out angle generally matched the test results, therefore the shell element aluminum honeycomb model can simulate the directional dependence of compressive strength of an actual aluminum honeycomb.

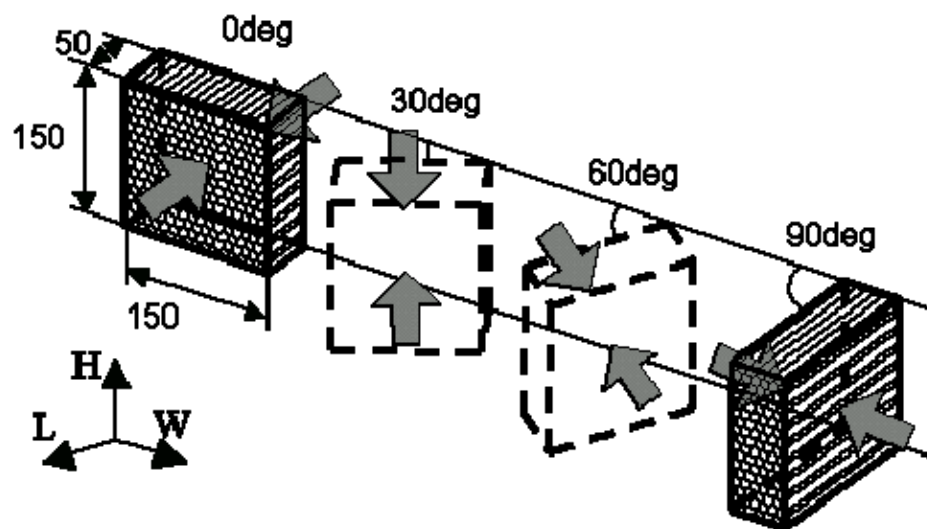


Fig.10 Concept of aluminum honeycomb compression test

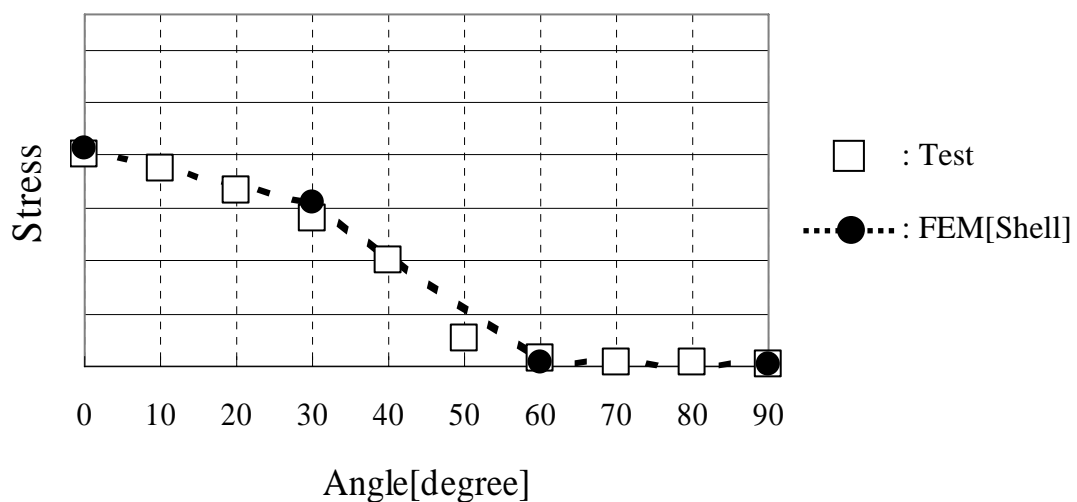


Fig.11 Relationship between test piece cutting angle and compressive stress

4.2 Comparison of test results and FEM analysis for barrier inspection

To verify the calculation accuracy of the newly created shell element ODB model, FEM analysis for barrier inspection was performed. Figure 12 shows the relationship between impactor stroke and barrier force in the FEM analysis for barrier inspection using an impactor, and Fig. 13 shows the deformed shape of the ODB after the collision.

The relationship between impactor stroke and barrier force in the shell element ODB model was examined. It was found that the stroke upon which the barrier force decreases differed slightly from the test results due to a difference in the rupture timing of the cladding sheet, but the force level was similar to the test result. In addition, when the core honeycomb in the shell element ODB model was examined, it was found that the core honeycomb was gathered to the impactor side due to the cladding sheet becoming entangled into the impactor. The result of shell element ODB model is more precise to the test result than solid element ODB model.

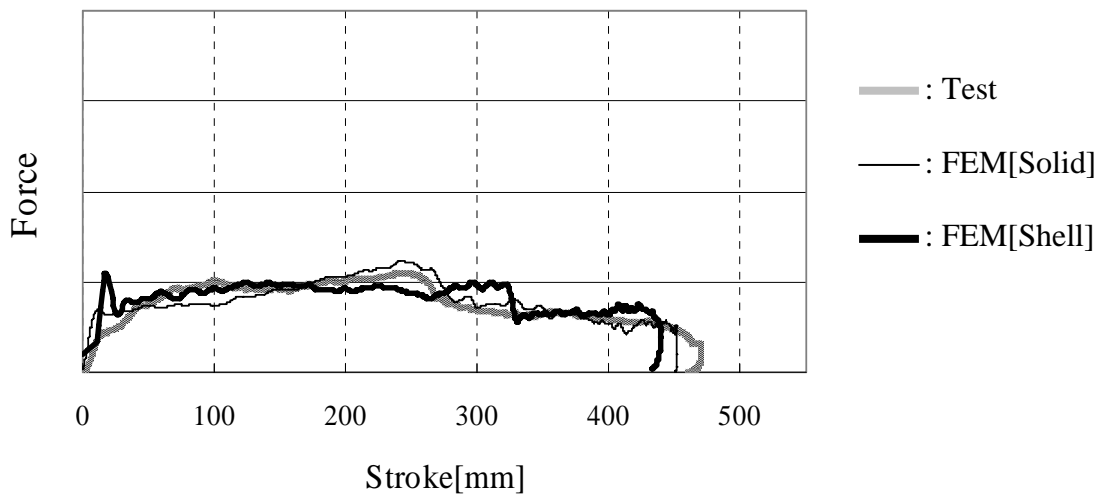


Fig.12 Comparison of Force-Stroke curves

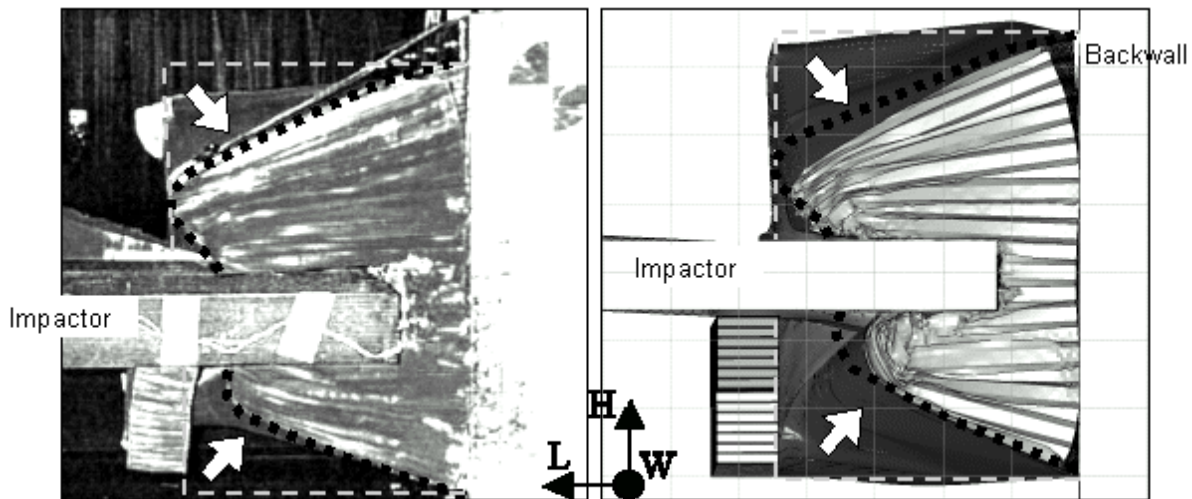


Fig.13 Deformed shape of ODB after impactor collision

4.3 Comparison of test results and FEM analysis for offset frontal collision

Offset frontal collision calculation was performed using a vehicle model and the shell element ODB model to verify the accuracy of the ODB model. Figure 14 shows the time history of the barrier force, and Fig. 15 shows the deformed shape of the vehicle after the collision.

The barrier force time history in the FEM analysis of the shell element ODB model shows that the peak level of force at $t=90$ ms is lower than with the solid element ODB model. In addition, when the remaining crushed portion of the vehicle upper member was compared, the difference with the test results decreased from 33 mm to 2 mm. The result of shell element ODB model is more precise to the test result than solid element ODB model.

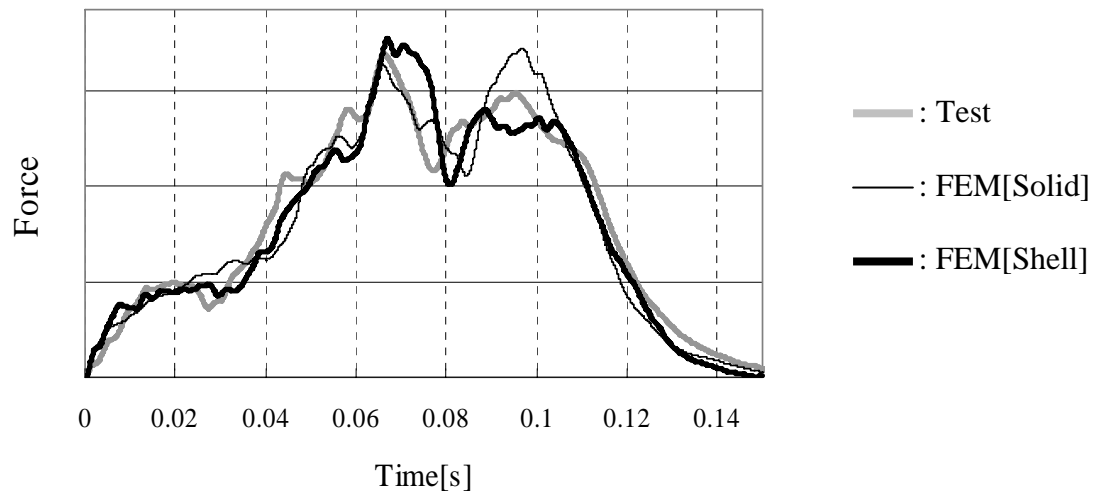


Fig.14 Time history of barrier force

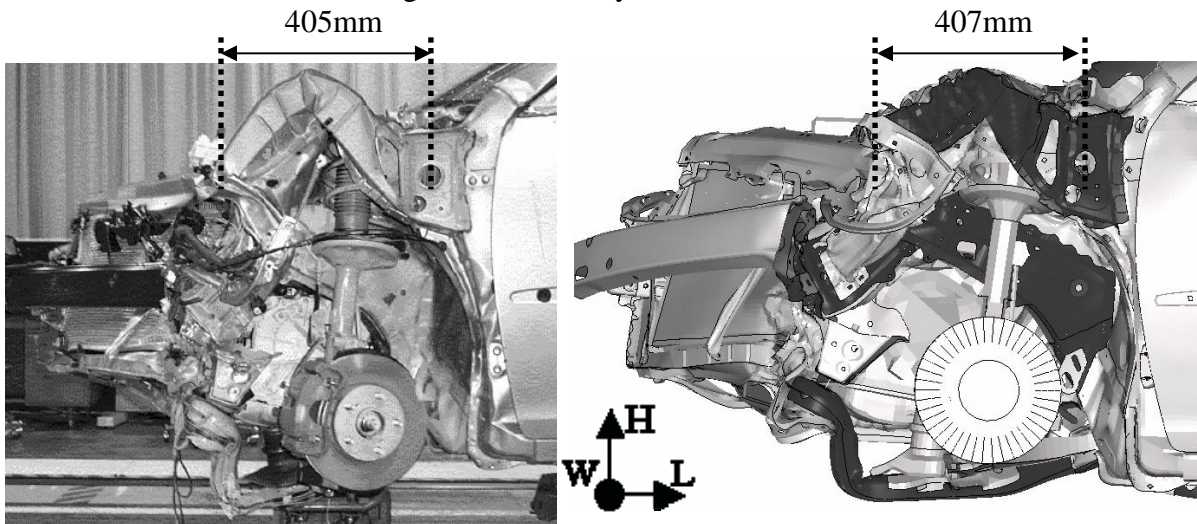


Fig.15 Deformed shape of vehicle after offset frontal collision

Figure 16 shows the deformed shape of the ODB after the collision. A comparison of the remaining crushed portion of the upper part of the ODB core honeycomb where the upper member collided showed that the difference with the test results decreased from 59 mm to 33 mm, which is better than the solid element ODB model. These results indicate that the calculation accuracy of the shell element ODB model is sufficient to predict vehicle deformation, the deformed shape of the barrier, and force time history in offset frontal collision analysis.

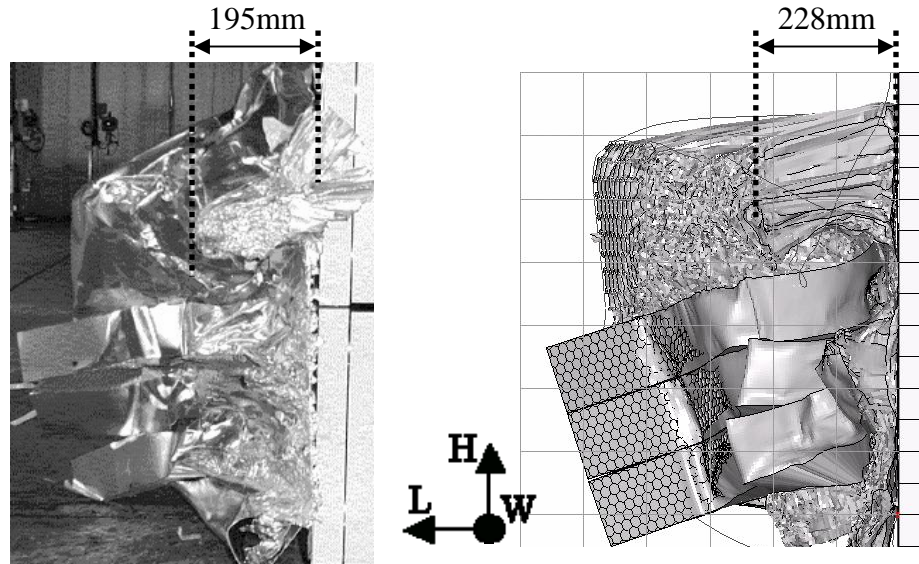


Fig.16 Deformed shape of ODB after offset frontal collision

5. Conclusion

A method of modeling aluminum honeycomb using shell elements has been successfully developed. This method was applied to ODB modeling, and barrier inspection analysis using an impactor and offset frontal collision analysis were performed. As a result, it was verified that this method is capable of simulating test results for vehicle and ODB deformed shapes, and for barrier force time history.

References

1. Dr. Tore Tryland, "Alternative Model of the Offset Deformable Barrier", 4th German LS-DYNA Forum 2005, Page. B-II-33_B-II-40
2. Robert Mayer, Scott Webb, J.T. Wang, Bill Liu, "Sled tests and simulations of offset deformable barrier", International Journal of Vehicle Safety Volume 1, Page. 238_251
3. Lei Hou, "Failure Modes Analysis in the Crash Barrier Simulation", 5th European LS-DYNA Users' Conference 2005, Page. 5b-02
4. Andreas Hirth, Paul Du Bois, Dr. Klaus Weimar, "A Material Model for Transversely Anisotropic Crushable Foams in LS-DYNA", 7th International LS-DYNA Users Conference, Page. 16-23_16-34
5. Tsuyoshi Yasuki, Noriko Watanabe, "Vehicle Crash Analysis Applications to a Vehicle Development", TOYOTA Technical Review Vol.51 No.1 Jun.2001, Page. 54_59
6. Koji Nojima, "Modeling and Accuracy of Offset Crash Deformable Barrier - Real phenomena and modeling technique ?", JSAE 2001, Page. 37_41
7. Moisey B Shkolnikov, "Honeycomb Modeling for Side Impact Moving Deformable Barrier(MDB)", 7th International LS-DYNA Users Conference, Page. 7-1_7-14
8. Abdullatif K. Zaouk and Dhafer Marzougui, "Development and Validation of a US Side Impact Moveable Deformable Barrier FE Model", 3rd European LS-DYNA Users Conference, Page. 14
9. Paul Du Bois, "Crashworthiness Engineering Course Notes"
10. J. Hallquist, "LS-DYNA Keyword Users Manual(Update), Version970/Rev5434"